J. Synchrotron Rad. (1998). **5**, 471–474

Advanced field-measurement method with three orthogonal Hall probes for an elliptically polarizing undulator

C.-S. Hwang,[a]* T. C. Fan,[a] F. Y. Lin,[a] Shuting Yeh,[a] C. H. Chang,[a] H. H. Chen[a] and P. K. Tseng[b]

[a]Synchrotron Radiation Research Centre, Hsinchu Science-Based Industrial Park, Hsinchu, Taiwan, and [b]Department of Physics, Tamkian University, Tamsuei, Taipei, Taiwan. E-mail: cshwang@alpha1.srrc.gov.tw

(*Received 4 August 1997; accepted 15 October 1997*)

A three-orthogonal-Hall-probe assembly with an 'on the fly' mapping method has been developed to characterize an elliptically polarizing undulator (EPU). The underlying design concept is that it can measure the three real field components without any field correction under a reliable and synchronization measurement method. Therefore, the relative central position shift, orthogonal angle and the planar Hall effect error between the three Hall probes should be calibrated and readjusted. Experimental results demonstrate that this method can yield an r.m.s. reproducibility of 10 G cm for the three field components and 2 G for the peak field strength. Under precision conditions this system can completely measure the three on-axis field components within 2 min for a 4 m-long EPU.

Keywords: elliptically polarizing undulators; three-orthogonal-Hall-probe assembly; planar Hall effect.

1. Introduction

Recent advances in developing and constructing an elliptically polarized undulator (EPU) (Sasaki *et al.*, 1993; Elleaume, 1990) have led to the production of right/left circularly polarized light. This polarized light can be used in experiments of magnetic circular dichroism in X-ray absorption, which are currently of great research interest and frequently involve metals of the first-row transition series. This magnet generates the horizontal magnetic field, B_x, and vertical field, B_y, as well as the longitudinal field, B_z. Therefore, a three-orthogonal-Hall-probe system is necessary for measuring the three magnetic field components. Our design concept is that the system can simultaneously measure the three real field components without any field correction. Therefore, to fulfil the design concept, the relative central position shift, orthogonal angle and the planar Hall effect error are calibrated and readjusted. Consequently, the relative central position shift on the vertical and horizontal transverse axes and the orthogonal angle of the three Hall probes are maintained within 0.12 mm and $90 \pm 0.2^\circ$, respectively. The planar Hall effect error is also controlled within 0.5 G.

is work presents a highly accurate calibration method for calibrating the uncertainty of the orthogonal angular error, planar Hall effect and central position shift. The calibration method requires a homogeneous magnetic field and a special field of the insertion-device magnet. A Hall-probe holder with an adjustable function is also deemed necessary. After calibration and adjustment, the three-orthogonal-Hall-probe system can obtain a real field distribution without any field strength modification, and performs a rapid speed measurement. Finally, field measurement results by a long-loop-coil method were used for double-checking the measurement results of this method. This comparison demonstrates that the maximum integral field errors between these two systems are within ± 20 G cm in a multipole-field-profile measurement.

2. Hall-probe holder design

A holder is designed for installing three orthogonal Hall probes (Siemens SBV613). According to the Hall-probe holder design concept, the three reference surfaces of the holder should be as orthogonal as possible. The Hall-probe centres can be installed in the holder's reference centre position. Several reference marks on the Hall-probe holder are used to align the tilt angle, surface plane and centres of the three Hall probes. Hence, the holder design should be an adjustable mechanism. This adjustable mechanism can be used to adjust the transverse axes central points into the same position, and easily adjust the Hall plane to be mutually orthogonal between each probe. (Notably, these adjustments should depend on the calibration results.)

The Hall probe can be fixed on the holder by plastic screws and plates (Hwang, 1997). The holder material is fibreglass to avoid thermal expansion and vibration. In this work the Hall-probe holder is installed on a rotor which is an adjustable mechanism having three degrees of freedom. Finally, three PT-100 thermoelements are installed in the holder and in direct contact with the three Hall probes to measure the Hall temperature.

3. Calibration algorithm

The calibration parameters include the magnetic field strength, the relative central position, the orthogonal angle and the planar Hall effect between the three Hall plates. The positions and angles can be precisely calibrated by the standard magnet and a high-quality field distribution of an insertion-device magnet. The first step of the calibration algorithm is to calibrate the field strength within 0.1 G and adjust the orthogonal angular error within $90 \pm 0.2^\circ$ in the standard magnet. The second step is to adjust the tilt angle of the three Hall probes on the holder to reduce the field error which is induced by the planar Hall effect. The third step is to calibrate and adjust the central position shift between each probe alternately. The three-dimensional Hall-probe calibration process is described below.

3.1. *Field strength calibration*

Three Hall probes with temperature sensors are installed on the same fixture. This fixture can be used to adjust the angle, θ (between the Hall plate and the magnetic field vector), of the three Hall probes individually (Hwang *et al.*, 1994). The fixture is put in the homogeneous-field standard magnet; the orthogonal angle, θ, of the three Hall probes is also adjusted until the three maximum field components have occurred. Next, the temperatures of the three Hall probes are recorded by the sensors of three PT-100 resistors. The temperature coefficient of the SVB613 Hall probe is -0.01%. Field strength calibration with respect to Hall voltage and temperature is then fitted by the two-dimensional splint fit method. Consequently, the accuracy of the field strength calibration can be controlled within ± 0.1 G.

3.2. *Orthogonal angle calibration*

After calibrating the field strength, the three Hall probes are installed in the Hall-probe holder. The orthogonal angular error, θ_{xy}, θ_{xz}, θ_{zx} and θ_{zy}, between each probe is readjusted and calibrated on the standard magnet. The first step involves aligning and adjusting the plane of the B_y probe perpendicular to the vertical field direction, and then recording the reference marks. θ_{xy} and θ_{zy} are then obtained by tuning θ_{xy} and θ_{zy} until the field strength of B_x and B_z is as close to zero as possible. Next, the probe holder is rotated 90° around the axis of the B_x probe to change the angle between the field direction and the Hall generator plane. The B_z probe is then perpendicular to the vertical field. The θ_{xz} and θ_{zx} values are then obtained by tuning θ_{xz} and θ_{zx} until the minimum and maximum field strength of the B_x and B_z probes have occurred individually. These procedures are repeated and readjusted alternately (Hwang, 1997) until the orthogonal angular error is within $90 \pm 0.2°$. Based on this method, the accuracy of the orthogonal angular calibration between each probe is adjusted to be (θ_{xy}, θ_{xz}, θ_{zx}, θ_{zy}) = (0.03, −0.15, −0.1, −0.18°). If a field correction is necessary, then these data can be inserted into the analysis code to reduce the field strength error.

3.3. *Planar Hall effect calibration*

After calibrating the orthogonal angle, the Hall-probe holder is carefully aligned with respect to the transverse x axis of the insertion-device magnet to reduce the tilt angle, φ, between the transverse component field, B_t, and the Hall current direction, I_c. If the planar Hall voltage is not neglected, then various methods (Berkes, 1992; Poole & Walker, 1981) can be used to calibrate the planar Hall voltage to keep the field error as small as possible in the three-dimensional magnetic field measurement. In our planar Hall effect calibration method (Hwang *et al.*, 1994; Hwang, 1997), the Hall-probe plane is adjusted to be parallel to the axis of the main homogeneous magnetic field direction. The Hall probe is then rotated around the axis of the Hall-generator plane to change the tilt angle, φ. Consequently, the planar Hall effect will produce a maximum field strength error at $\varphi = 45°$. However, the planar Hall coefficient in our Siemens SBV613 Hall generator is extremely small. (This Hall generator is a high-doped semiconductor with small resistivities; unfortunately, Siemens no longer manufacture it.) Hence, the field strength error induced from the planar Hall effect can be kept extremely small (Berkes, 1992; Hwang *et al.*, 1994; Braunersreuther, 1978). In particular, the tilt angle, φ, of our Hall plate can be maintained within 50 mrad. Therefore, the field strength error induced from the planar Hall effect is maintained within 0.5 G at the transverse field $B_t = 1$ T.

3.4. *Hall-probe centre calibration*

The Hall-probe centres can be installed at the common vicinity point of the transverse horizontal and vertical axes by means of the holder reference plane. The reference plane can maintain the centre shift within ±0.5 mm between each probe. The relative central position shift on the midplane is calibrated by the sinusoidal field distribution of the magnetic field features of an insertion device. The calibration accuracy is within ±0.05 mm.

The three probes are fixed above (below) the lower (upper) jaw at $x \neq 0$ and then the field distribution is scanned along the longitudinal z axis. Therefore, the relation of the z-axis central position between the B_y, B_x and B_z probes ($x \neq 0$) is found at z = 0 (where $B_z = 0$) and $z = \lambda_u/4$ (where $B_y = 0$ and $B_x = 0$). If the B_y and B_x probes are fixed above (below) the lower (upper) jaw at z = 0 (z = 0 means the central pole region) and the B_z probe at $z = \lambda_u/4$, then the three probes scan the field distribution along the x axis. Consequently, the central position on the x axis between the three probes is found at $x = 0$ (where B_y and B_z have a maximum value and $B_x = 0$). Finally, adjusting the insertion device allows it to become a pure vertical field. If the B_z probe is placed at $z = \lambda_u/4$, $x = c$, and the B_x and B_y probes are placed at $z = 0$, $x = c$, then the three probes scan the field distribution along the y axis, where c is about 7/8 of the pole width. Consequently, the central positions of the three probes are found at $y = 0$ (where B_y has a minimum value and $B_x = B_z = 0$). The central positions of the relative x and y axes for the three probes verify that the central position shift can be maintained within 0.12 mm (Hwang, 1997).

4. Mapping system

The main control unit is based on a PC, and the system control and data acquisition cards are installed in the PC slot. Fig. 1 depicts the hardware architecture. The software was developed using the *LabView* program. The scan range in the longitudinal direction can be adjusted *via* two limit switches at both sides of the granite. Before measurement, the AT-MIO-16X sends an external trigger to reset the divide by circuit. Next, the Hall probe begins to scan along the z axis until the xy stage touches the return limit switch. The optical linear scalar sends one signal per 0.4 mm to trigger the AT-MIO-16X for sampling the voltage of the three Hall probes alternately. Consequently, the elementary step distance of each magnetic field component is 1.2 mm. The xy stage, upon touching the return limit switch, returns to the starting limit switch position where the linear encoder sends a reference signal to determine the absolute position. In the return interval time, the temperatures of the three Hall probes are recorded by the PT-100 thermoelements *via* DVM to conserve the time consumption. Meanwhile, the recorded data are transferred from the AT-MIO-16X buffer to the hard disk. The xy stage will position the probe on the transverse axes automatically when the longitudinal direction scan is completed.

5. System precision

The magnetic field is measured by moving the three-orthogonal-Hall-probe assembly along the axes of the EPU and APU magnet, and then recording the B_x, B_y and B_z magnetic field strengths as a function of the longitudinal and transverse posi-

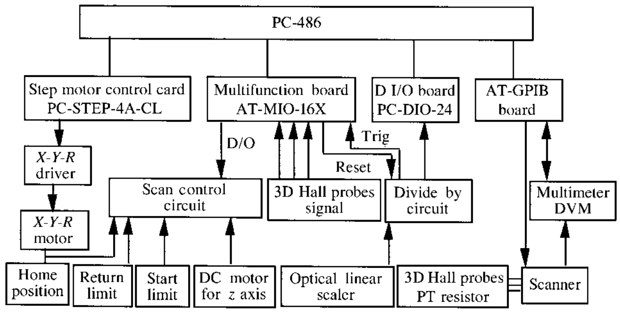

Figure 1
The hardware architecture of the three-orthogonal-Hall-probe system with the 'on the fly' mapping method.

tions. This measurement and analysis of the results can reflect the multipole integral field behaviour of the EPU magnet. The experimental results of the reproducibility on the transverse axis on the EPU are shown in Fig. 2. According to this figure, an r.m.s. reproducibility of 10 G cm for the three field components can be achieved in the multipole field mapping. A long-loop-flipping-coil measurement system is also used to measure the multipole integral field distribution under the same conditions as for the Hall-probe measurement. Fig. 3 confirms not only that the two systems closely correspond to each other, but also that the maximum integral field error between the Hall-probe and long-loop-coil systems is around 135 ± 20 G cm of B_x and ±20 G cm of B_y. In our laboratory the earth field $B_x \simeq 0$ G and $B_y \simeq 0.25$ G. Hence, if considering the earth field strength, the exact absolute field strength difference between these two systems is around 135 G cm of B_x and 105 G cm of B_y (the measurement ranges of the three-dimensional Hall-probe and long-loop-coil systems are 1.2 m and 5.5 m, respectively). There is the same amount of absolute field strength difference in the two components of B_x and B_y. Therefore, the difference may come from the calibration error of these two systems.

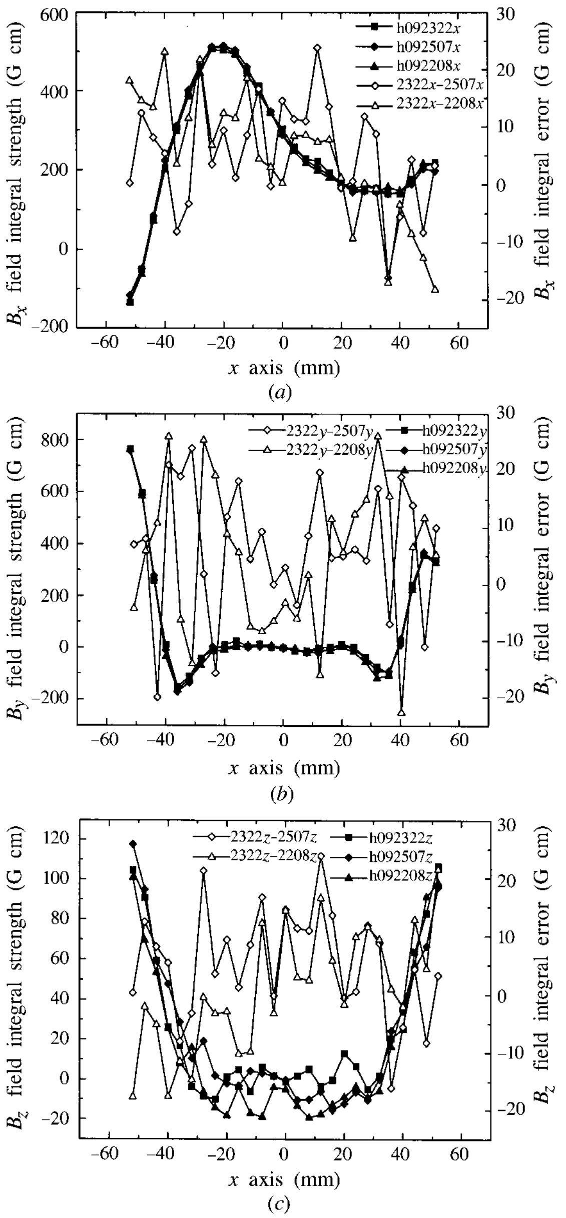

Figure 2
The transverse field distribution of (*a*) $B_x(x)$, (*b*) $B_y(x)$ and (*c*) $B_z(x)$ as repeatedly measured by the three-dimensional Hall-probe system.

6. Conclusions

This study presents an 'on the fly' mapping method with a three-orthogonal-Hall-probe mapping system to enhance the measurement speed and perform a real field measurement without any field correction. The proposed method is deemed necessary for a long insertion device, particularly for the EPU measurement. The method proposed herein can measure the on-axis fields of the three components within 2 min for a 4 m-long insertion device. In addition, the magnetic field calibration method can fulfil the demands of the measurement concept. Based on this method, although a ±0.5 mm uncertainty in the position shift occurs between the three orthogonal Hall probes, the position shift can be reduced within 0.12 mm; the orthogonal angular error between the three Hall probes can be calibrated within 90 ± 0.2°. If a field correction is necessary, the calibration data can be inserted into the analysis code for modifying the field error. Finally, the planar Hall effect of our Hall probe can also be controlled within 0.5 G by carefully aligning the tilt angle between the transverse field and the Hall current direction.

The authors are indebted to Director C. T. Chen and Dr J. R. Chen (SRRC) for supporting this project. SRRC staff members J.

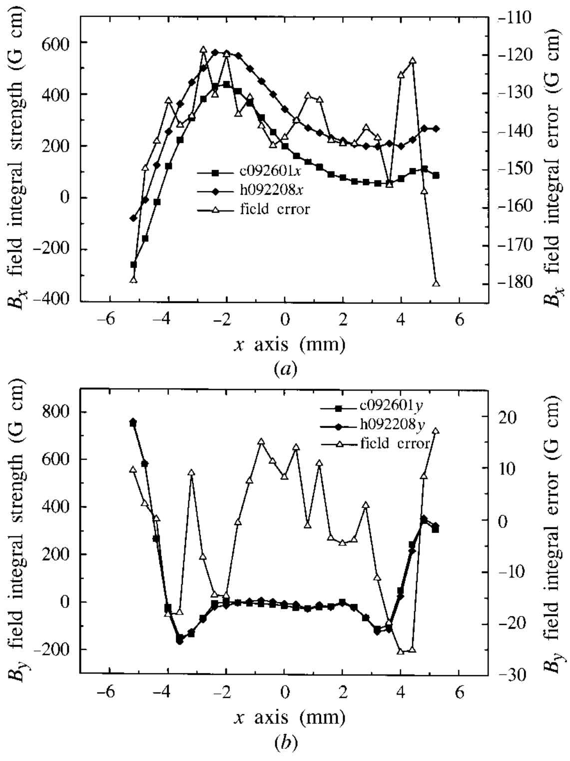

Figure 3
The transverse field distribution of (*a*) $B_x(x)$ and (*b*) $B_y(x)$ as measured by the three-dimensional Hall-probe system and the long-loop-flipping-coil system.

Y. Hsu and K. H. Chen are also commended for their technical assistance.

References

Berkes, B. (1992). CERN Accelerator School (CAS), CERN-92–05, pp. 167–192. CERN, Switzerland.

Braunersreuther, E. (1978). CERN PS-CD Note 78–3. CERN, Switzerland.

Elleaume, P. (1990). *Nucl. Instrum. Methods*, A**291**, 371–377.

Hwang, C. S. (1997). PhD thesis, University of Chiao Tung, Taiwan.

Hwang, C. S., Lin, F. Y., Huang, T. H., Jan, G. J. & Tseng, P. K. (1994). *Rev. Sci. Instrum.* **65**(8), 2548–2555.

Poole, M. W. & Walker, R. P. (1981). *IEEE Trans. Magn.* **17**, 2129–2132.

Sasaki, S., Kakuno, K., Takada, T., Shimada, T., Yanagida, K. & Miyahara, Y. (1993). *Nucl. Instrum. Methods*, A**331**, 763–767.